

Calculations of quantum oscillations in cuprate superconductors considering the pseudogap

E. V. L. de Mello¹

¹*Instituto de Física, Universidade Federal Fluminense, 24210-346 Niterói, RJ, Brazil**

The observations of quantum oscillations in overdoped cuprate superconductors were in agreement with a charge density contained in a cylindrical Fermi surface but the frequencies of lightly doped compounds were much smaller than expected. This was attributed to a topological transition into small pockets of Fermi surface associated with the existence of the charge density wave underlying superlattice. On the other hand, spectroscopic measurements suggested that the large two-dimensional Fermi surface changes continuously into a set of four disconnected arcs. Here we take into account the effect of the pseudogap that limits the available k -space area where the Landau levels are developed on the Luttinger theorem and obtain the correct carrier densities. The calculations show how the disconnected arcs evolve into a closed Fermi surface reconciling the experiments.

The details of different Fermi surfaces in metals have long been explored by quantum oscillations experiments (QO), like conventional de Haas-van Alphen effect. The quantum oscillations are a direct consequence of the quantization of closed Landau orbits perpendicular to an applied magnetic field. The energy of a given orbit depends on the applied field, and varying the field, there is always a resonance when a Landau level crosses the Fermi energy, from which the transverse (to the field) area of the Fermi surface is derived. The QO in the overdoped cuprate superconductor $\text{Ti}_2\text{Ba}_2\text{CuO}_{2+\delta}$ (Ti2201) show the existence of a large Fermi surface covering nearly two-thirds of the Brillouin zone¹ in very good agreement with the angle-resolved photoemission spectroscopy (ARPES) results². The frequency (F) of oscillation is related with cross-sectional area $A_{\mathbf{k}}$ of the Fermi surface by the Onsager relation, $A_{\mathbf{k}} = 2\pi eF/\hbar$. Assuming that the Fermi surface is strictly two-dimensional, then the carrier density per plane per area is given by Luttinger's theorem; $n = 2A_{\mathbf{k}}/A_{\text{BZ}} = 1 + p$, where $A_{\text{BZ}} = (2\pi/a)^2$ is the BZ area, p is the average doping or hole density and a the lattice parameter. These relations work quite well with several overdoped Ti2201 compounds^{1,3} with $p \approx 0.25 - 0.30$.

However QO measurements in underdoped $\text{YBa}_2\text{Cu}_3\text{O}_y$ (Y123) and in $\text{HgBa}_2\text{CuO}_{4+y}$ (Hg1201) are both 25-32 times lower than the overdoped Ti2201 frequency^{4,9}, implying, by the Onsager relation, in very small cross-sectional areas $A_{\mathbf{k}}$. Consequently, there is a discrepancy with Luttinger theorem since typical doping differences are lower only by a factor of 2-3. To explain this overdoped/underdoped difference it was proposed a Fermi surface reconstruction into several small pockets of Fermi surface⁴⁻⁹. The change of sign in the Hall resistances with the temperature in high magnetic-field-induced normal state of (Y123) and on Hg1201 suggested that these pockets are electron-like rather than hole-like^{10,11}. Since the negative Hall resistances occur between $p = 0.07 - 0.15$ ¹², their existence and the crossover between electron-hole pockets were attributed to the incommensurate charge order (CO) phase^{10,13} or charge density waves (CDW) superlattice formation¹⁴.

In order to check this Fermi surface reconstruction crossover an effort was made to perform angle resolved photoemission spectroscopy (ARPES) experiments with Y123¹⁵ and Hg1201¹⁶, but they both did not detected the presence of electron pockets. Thus, the interpretation of QO in terms

of electron and hole pockets differs markedly from single-particle spectroscopy, suggesting that high magnetic fields might induce a new electronic state.

We provide a new interpretation to QO taking into account the charge instabilities on Luttinger theorem, that was originally derived in the context of a Fermi liquid with uniform density. In previous papers¹⁷⁻¹⁹ we discussed the large amount of experimental evidences for spontaneous symmetry breaking and anomalous long-range ordered electronic states arising near the PG temperature $T^*(p)$. The correlations between charge modulations wavelengths Q_{CO} ($= 1/\lambda_{\text{CO}}$) in real space and the distance between the Fermi arcs tips in k -space that is dominated by the PG was established by scanning tunneling microscopy (STM)^{20,21} and by a combination of ARPES, STM and resonant x-rays (REXS) on $\text{Bi}_2\text{Sr}_{2-x}\text{La}_x\text{O}_{6+\delta}$ (Bi2201)²². On the theoretical side, we demonstrated that the PG energy $\Delta_{\text{PG}}(p)$ is proportional to the ground state energy of a two-dimensional potential well with radius equal to $\lambda_{\text{CO}}(p)$ ¹⁹, establishing a direct connection between the CO spatial scale and the PG energy $\Delta_{\text{PG}}(p)$. The charge anomalies are strong evidence of a non-Fermi liquid behavior and pose the question of how does it affect the Luttinger theorem? We shall answer this question in the next paragraphs.

Another important ingredient comes from measurements of the momentum or wave vector direction like Raman scattering^{23,24} and ARPES²⁵ that established the d -wave symmetry of the $\Delta_{\text{PG}}(p)$. We simulate the CO anomalies by a Cahn-Hilliard approach in real space that is quite precise in reproducing the experimental observations^{17,18,26,27}. In Fig. 1(a) we show an example of simulation; the $p = 0.15$ compound from the Bi2212 family exhibiting CO with checkerboard structure in 100 vs. 100 unit cells. In Fig. 1(b) we show the two-dimensional k -space single particle energy $\Delta_{\text{PG}}(k_x, k_y) = \Delta_{\text{PG}}(p, T)|\cos(k_x a) - \cos(k_y a)|/2$. These two maps show the charge modulations and the PG effects on cuprates in real and momentum space what are two forms of the same phenomenon and must be taken simultaneously in the Luttinger theorem.

The SC order parameters are formed in the alternating (high and low) charge density domains that are connected by local Josephson coupling or superfluid phase stiffness ρ_{sc} . On the other hand, under the QO conditions, applied fields around 50 T and temperature $T \approx 1$ K, the Cooper pairs break down and

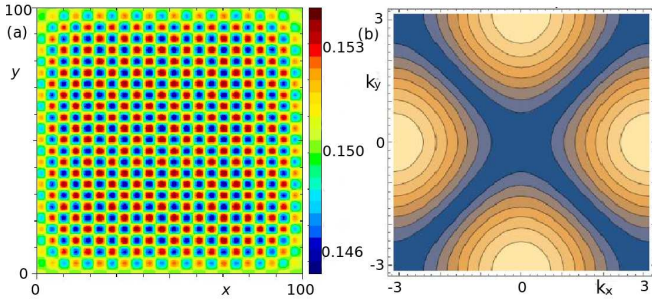


FIG. 1. The effect of the PG in real and k -space. (a) The Bi2212 compound with $p = 0.15$ density map with the formation of a CDW with hole-rich domains in red and hole-poor in blue. In (b) we show the energy cuts of the d -wave pseudogap $|\Delta_{PG}(k_x, k_y)|$ which vanishes at the diagonals or nodal directions and is maximum at the antinodes.

the superfluid density n_{sc} become low energy normal carriers on the top of the Fermi surface. But n_{sc} is directly proportional to the superfluid phase stiffness ρ_{sc} that determines the energy scale or available kinetic energy of these unpaired holes. In opposition to this behavior, the PG or the charge instabilities like CDW are unaffected by large magnetic fields as demonstrated, for instance, by Chang *et al*²⁸. Consequently, the free carriers from unpaired holes are constrained by the PG and their low energies to stay in the area near the BZ diagonals where

$$\rho_{sc}(p, T = 0 \text{ K}) \geq |\Delta_{PG}(k_x, k_y)|. \quad (1)$$

This inequality defines the 2D area or *restricted BZ area* (RBZ(p)), that are shown in Fig. 2(a) for electrons and Fig. 2(b) for holes of three compounds with $p = 0.10, 0.12$ and 0.27 together with the Fermi level of Tl2201 with $p = 0.27$, just for reference. The full BZ area is $(2\pi/a)^2 = 265 \text{ nm}^{-2}$ with the lattice parameter $a = 0.365 \text{ nm}$ and the RBZ(p) area of these three compounds are calculated by a Mathematica program and given in Table I.

Several experiments compiled by Ref.[23] are indicative that the low temperature $\Delta_{PG}(p, 0)$ decreases linearly with p . Thus in the far overdoped region $\Delta_{PG}(p, 0) \rightarrow 0$ and it does not touch the overdoped Tl2201 Fermi level. In this case the Landau levels at the Fermi surface are almost perfect circles, like the Tl2201 with $p = 0.27$ shown by the red curve in Fig. 2(b). Therefore for $p \geq 0.27$ the Landau levels near the Fermi surface are similar to those of Fermi liquids. For $p < 0.27$, according our criteria of $\rho_{sc}(p, T = 0 \text{ K}) \geq |\Delta_{PG}(k_x, k_y)|$, the Landau levels become continuously into four large arcs that almost fulfill a complete circle, but the arcs diminish with p and eventually vanish. Therefore the low energy holes near the Fermi level form Landau levels around the arcs confined at the nodal or diagonal directions as it is the case for $p = 0.10$ and 0.125 displayed in Fig. 2(a) and (b).

Consequently, the measured QO frequencies F on underdoped samples are from the carrier oscillations around these four squeezed red circles or ellipsoids shown in Fig. 2(a) and (b) having total area $A_k(p)$ given by the Onsager relation. Taking all the above conditions we rewrite Luttinger theorem

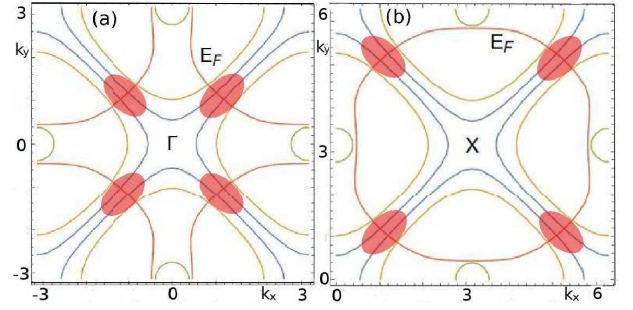


FIG. 2. Low temperature d -wave PG $|\Delta_{PG}(k_x, k_y)|$ for $p = 0.10, 0.125$ and 0.27 . (a) Electron and (b) hole Fermi surface E_F for $p = 0.27$ for comparison. At this doping the PG is very small, barely touches the Fermi surface and E_F is similar of free electrons. When the PG becomes stronger, like for $p = 0.10$ and 0.125 shown in the plots, it cuts the Fermi surface near the antinodal regions and the low energy Landau levels are restricted to these regions, like the squeezed red circles or ellipsoids shown in the figure.

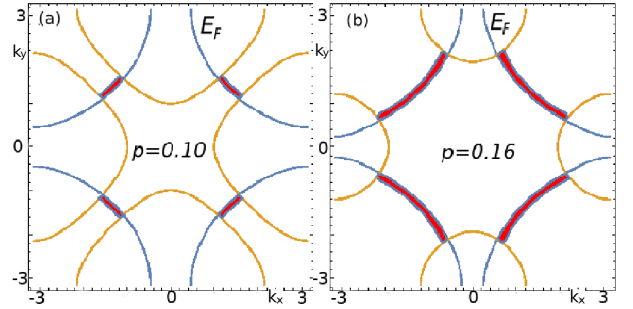


FIG. 3. The d -wave SC amplitude $|\Delta_{sc}(k_x, k_y)|$ at $T \approx T_c + 10 \text{ K}$. The same functional form of the PG and SC gap is an additional evidence of the connection between them. At these temperatures the size of the Fermi arcs or gapless regions are determined by thermal and quantum phase fluctuations, they increase and cover the whole Fermi surface when $T \rightarrow T^*$. To calculate the gapless arc sizes it is needed to take these two fluctuation effects into consideration like the derivations for three Bi2212 compounds in Fig. 6 of Ref. 18, after ARPES measurements³².

as:

$$n = 1 + p = A \times 2A_k(p)/\text{RBZ}(p), \quad (2)$$

where $A = 1$ for $p \geq 0.27$ and 4 otherwise. We calculate RBZ(p) with the zero temperature $\Delta_{PG}(p, 0)$ ²³ and $\rho_{sc}(p, 0)$ from our previous paper²⁹ in agreement with experiments³⁰. The $\Delta_{PG}(p, 0)$ and $\rho_{sc}(p, 0)$ values used in the calculations for $p = 0.09$ (Hg1201), $0.10, 0.125$ (Y123) and $p = 0.30$ (Tl2201) are all listed in Table I. We do not have data to calculate $\rho_{sc}(0.09)$ for Hg1201 and we used that of Bi2212 in the preceding paper²⁹ because their similar $T_c(p)$ curves. It is known that $\rho_{sc}(p, 0)$ is maximum near or further the optimum doping and is small in the underdoped region while $\Delta_{PG}(p, 0)$ decreases linearly with p . Both effects combined imply that RBZ(p) decreases rapidly as p goes down below $p \leq 0.16$ and are much less than the full BZ area also listed in Table I. Using the areas $A_k(p)$ derived from the QO measured frequencies F by the Onsager relation and Eq. (2), we

TABLE I. We list the data and calculations of the four compounds used in QO⁴⁻⁹. The measured frequencies in the third column are in tetrahertz (T). $\rho_{\text{sf}}(0)$ for Y123 is from the previous paper²⁹, Tl1201 is from experiments³⁰ and the value of Hg1201 is assumed to be close to that of Bi2212²⁹. The calculated densities from Eq. 2 are in the last column and in agreement with the experimental values of column 1.

p	T_c	F(T)	A_k (nm ⁻²)	Δ_{PG} (meV)	$\rho_{\text{sc}}(0)$ (K)	RBZ nm ⁻²	$1 + p$ (Eq. 2)
0.10 (Y123)	57 K	530 \pm 20T[4]	5.10	100.0 meV [23]	87.5	36.89	1.106
0.125 (Y123)	64 K	660 \pm 15T[5 and 6]	6.37	91.0 meV[23]	92.5	45.26	1.126
0.090 (Hg1201)	72 K	840 \pm 30T [8]	8.08	100.0 meV [31]	143.4	59.2	1.091
0.30 (Tl2201)	10 K	18100 \pm 50T [1]	172.8	4 meV [23]	29.5	265	1.303

derive hole doping densities in very good agreement with all the compounds used in the QO experiments^{1,3-9} as listed in Table I.

It is important to emphasize that the Landau levels at the Fermi surface in the presence of the PG provides an explanation to the existence of the four hole pockets with the measured frequencies or areas. Our approach is also in qualitative agreement with the Fermi arcs measured by several ARPES experiments in the absence of a magnetic field and finite temperature^{2,20,32-36}. We have previously demonstrated¹⁸ that the Fermi arcs become finite at $T > T_c$ due to thermal and quantum fluctuations of the local superconducting order parameter phase Φ_j . We have shown that the superconducting amplitude is finite but the order parameter vanishes along the nodal direction due to average quantum and thermal phase fluctuations¹⁸. In Fig. 3 we show these phase fluctuation cal-

culations for $p = 0.10$ (a) and 0.16 (b) at $T \approx T_c + 10$ K that reproduced ARPES measurements on Bi2212³².

In summary, we showed how to obtain the hole density in the QO experiments of several underdoped compounds from two well known properties: *i*- The absolute values of the PG at low temperature, $\Delta_{\text{PG}}(p, 0)$ that constraint low energy particles in k -space. *ii*-The superfluid phase stiffness $\rho_{\text{sf}}(p, 0)$ that sets the free carriers from Cooper pairs energies. In this manner we obtain the k -space energetically favorable area where the low energy unpaired holes form Landau levels on the top of the Fermi surface. The calculations provided clearly quantitative results listed in Table I, a new interpretation to the QO experiments and indicate a way to reconciled these observations with the Fermi arcs measurements by ARPES.

I acknowledge partial support by the Brazilian agencies CNPq and FAPERJ.

* Corresponding author: evandro@mail.if.uff.br

¹ B. Vignolle *et al.*, Nature **455**, 952 (2008).

² M. Platé *et al.*, Phys. Rev. Lett. **95**, 077001 (2005).

³ A. F. Bangura *et al.*, Phys. Rev. B **82**, 140501 (2010).

⁴ N. Doiron-Leyraud *et al.*, Nature **447**, 565 (2007), 0801.1281.

⁵ A. F. Bangura *et al.*, Phys. Rev. Lett. **100**, 047004 (2008).

⁶ E. A. Yelland *et al.*, 10.1103/PhysRevLett.100.047003.

⁷ C. Jaudet *et al.*, Physical Review Letters **100**, 187005 (2008).

⁸ N. Barišić *et al.*, Nature Physics **9**, 761 (2013).

⁹ M. K. Chan *et al.*, Nature Communications **7** (2016).

¹⁰ D. LeBoeuf *et al.*, Nature **450**, 533 (2007).

¹¹ N. Doiron-Leyraud *et al.*, Physical Review X **3**, 1 (2013).

¹² S. Badoux *et al.*, Nature **531**, 210 (2016).

¹³ L. Taillefer, Journal of Physics: Condensed Matter **21**, 164212 (2009).

¹⁴ S. Chakravarty, Science **319**, 735 (2008).

¹⁵ M. A. Hossain *et al.*, Nature Physics **4**, 527 (2008).

¹⁶ I. M. Vishik *et al.*, Physical Review B **89**, 1 (2014).

¹⁷ E. V. L. de Mello, Europhys. Lett. **99**, 37003 (2012).

¹⁸ E. V. L. de Mello and J. E. Sonier, Phys. Rev. B **95**, 184520 (2017).

¹⁹ E. V. de Mello, (2019), submitted paper.

²⁰ K. M. Shen *et al.*, Science **307**, 901 (2005).

²¹ W. D. Wise *et al.*, Nature Physics **4**, 696 (2008).

²² R. Comin *et al.*, Science (New York, N.Y.) **343**, 390 (2014).

²³ S. Huefner, M. A. Hossain, A. Damascelli, and G. A. Sawatzky, Rep. Prog. Phys. **71**, 062501 (2007).

²⁴ N. Munnikes *et al.*, Phys. Rev. B **84**, 144523 (2011).

²⁵ A. Damascelli, Z. Hussain, and Z.-X. Shen, Rev. Mod. Phys. **75**, 473 (2003).

²⁶ E. V. L. de Mello, R. B. Kasal, and C. A. C. Passos, J. Phys.: Condens. Matter **21**, 235701 (2009).

²⁷ E. V. L. de Mello and R. B. Kasal, Physica C: Superconductivity **472**, 60 (2012).

²⁸ J. Chang *et al.*, Nature Physics **8**, 871 (2012).

²⁹ E. V. de Mello, Submitted paper.

³⁰ C. Niedermayer *et al.*, Phys. Rev. Lett. **71**, 1764 (1993).

³¹ Y. Li *et al.*, Phys. Rev. Lett. **111**, 187001 (2013).

³² W. S. Lee *et al.*, Nature **450**, 81 (2007).

³³ M. R. Norman *et al.*, Nature **392**, 157 EP (1998).

³⁴ T. Yoshida *et al.*, Phys. Rev. B **74**, 224510 (2006).

³⁵ A. Kanigel *et al.*, Nature Physics **2**, 447 (2006).

³⁶ T. Yoshida, M. Hashimoto, I. M. Vishik, Z.-X. Shen, and A. Fujimori, J. Phys. Soc. Japan **81**, 011006 (2012).